Supplementary Online Content

Ecker C, Andrews DS, Gudbrandsen CM, et al; Medical Research Council Autism Imaging Multicentre Study (MRC AIMS) Consortium. Association between the probability of autism spectrum disorder and normative sex-related phenotypic diversity in brain structure. *JAMA Psychiatry*. Published online February 8, 2017. doi:10.1001/jamapsychiatry.2016.3990

This supplementary material has been provided by the authors to give readers additional information about their work.

eTable 1. Frequency Ratios of ASD Cases to TD Controls, and Males to Females, Acquired Within and Across the Different Acquisition Sites

		Group		
		ASD	Control	total
Cambridge	female	28	28	56
	male	25	26	51
London	female	21	19	40
	male	24	25	49

eTable 2. Population Prevalence of ASD for Biological Males and Females With Male or Female Neuroanatomical Brain Phenotype

	S = 1		S = 0	
	N = 1	N = 0	N = 1	N = 0
D = 1	0.025	0.017	0.013	0.002
D = 0	0.975	0.983	0.987	0.998

Note. D: diagnosis of ASD (0=no, 1=yes), S: biological sex/gender (0=female, 1=male), N: neuroanatomical brain phenotype (0=female, 1=male); Notably, the probability of receiving a diagnosis of ASD appears to increase for male participants with N=0. This is due to the fact that the probability of being classified as N=0 for biological males is relatively low, thereby inflating the conditional probability of having ASD.

eTable 3. Differences in Neuroanatomical Patterns Associated With High Probability of ASD Between Men and Women

				Talairach				
ID	Region Labels	Side	BA	*x*	*y*	*z*	t_{max}	$p_{cluster}$
Females > Males								
1	banks superior temporal sulcus, caudal middle frontal gyrus, inferior parietal cortex, insula, lateral, orbital frontal cortex, middle temporal gyrus, pars opercularis, pars triangularis, postcentral gyrus, precentral gyrus,rostral middle frontal gyrus, superior temporal gyrus	R	11/22/44/45/46	34	-25	14	4.96	6.09×10^{-6}
2	cuneus cortex, fusiform gyrus, isthmus-cingulate cortex, lingual gyrus, precuneus cortex	L	18/19/20/30/31/37	-32	-48	-16	3.78	6.29×10^{-6}
3	insula, lateral orbital frontal cortex, pars opercularis, pars triangularis, postcentral gyrus, precentral gyrus, supramarginal gyrus	L	11/45/47	-38	-18	16	4.57	1.37×10^{-5}
4	inferior parietal cortex, supramarginal gyrus	R	19/39/40	41	-66	43	4.54	1.35×10^{-3}
5	fusiform and lingual gyrus, parahippocampal gyrus	R	19/20/37	24	-44	-7	3.47	1.09×10^{-2}
6	caudal anterior-cingulate cortex, medial orbital frontal cortex, rostral anterior cingulate cortex, superior frontal gyrus	L	25/32/24	-12	42	8	4.45	1.27×10^{-2}
7	caudal anterior-cingulate cortex, paracentral lobule, posterior-cingulate cortex, precuneus cortex, superior frontal gyrus	L	24	-13	-15	38	3.97	1.34×10^{-2}

8	postcentral gyrus, superior parietal cortex	L	7	-27	-55	60	3.25	4.05×10^{-2}

Note. BA, Brodman Area; tmax, maximum absolute t value within cluster, x,y,z, Talairach coordinates at tmax; pcluster, cluster probability; R, right; L, left

eTable 4. Results of the Vertex-wise Analysis of CT Utilizing a General Linear Model (GLM)

				Talairach				
ID	Regional Labels	Side	BA	*x*	*y*	*z*	t_{max}	$p_{cluster}$
Group-by-Sex Interaction								
(1)	fusiform gyrus, inferior/middle temporal gyrus, lingual gyrus, parahippocampal gyrus	L	19/20/34/35/37/38	-29	-71	-5	3.29	3.5×10^{-6}
(2)	fusiform gyrus, inferior temporal gyrus, lateral occipital cortex, lingual gyrus, parahippocampal gyrus	R	18/19/34/35/37	26	-27	-18	3.42	5.49×10^{-4}
(3)	superior temporal sulcus, middle temporal gyrus	R	21/22	60	-33	-6	3.51	2.13×10^{-2}
Contrast: ASD males > TD males								
(1)	fusiform gyrus, inferior/middle temporal gyrus	L	18/19/20/37	-52	27	-19	2.61	1.04×10^{-2}
(2)	fusiform gyrus, lateral occipital cortex, lingual gyrus, parahippocampal gyrus	R	18/19/37	29	-60	-8	2.71	2.90×10^{-2}
Contrast: ASD females < TD females								
(1)	entorhinal cortex, fusiform gyrus, inferior/middle temporal gyrus, lingual gyrus, parahippocampal gyrus	L	18/19/20/34/35/37/38	-30	-69	-6	-3.90	2.23×10^{-6}
(2)	entorhinal cortex, fusiform gyrus, inferior/middle temporal gyrus, lateral occipital cortex, lingual gyrus, parahippocampal gyrus	R	18/19/20/34/35/36/37	25	-26	-18	-4.13	1.08×10^{-6}
(3)	superior temporal sulcus/gyrus, inferior parietal cortex, middle/superior temporal gyrus	R	21/22/39	62	-33	-6	-3.61	1.08×10^{-3}

(4)	insula, pre-/post-central gyrus, supramarginal gyrus	L	40/41	-44	-18	16	-3.96	1.23×10^{-2}
(5)	insula, pre-/post-central gyrus, superior temporal gyrus, supramarginal gyrus	R	40/41	46	-14	20	-3.67	4.17×10^{-2}

Note. ID, cluster number; BA, approximate Brodman Area; t_{max}, maximal *t* test statistic within cluster, *x*,*y*,*z*, Talairach coordinates at t_{max}; $p_{cluster}$, cluster probability; R, right; L, left

eTable 5. Differences in Demographic Measures Between Diagnostic Groups and Biological Sexes

	Groups			
	ASD (*n*=98)	Control (*n*=98)	*F*(*df*=1)	*p*
Age [years]	26.88 ± 7.18	27.39 ± 6.44	0.099	0.585
Full-scale IQ (WASI)	113.74 ± 12.31	116.44 ± 9.48	3.142	0.078
Verbal IQ	113.52 ± 12.89	113.68 ± 10.75	0.027	0.871
Performance IQ	111.28 ± 14.02	115.61 ± 9.75	6.179	0.014*
Mean Cortical Thickness [mm]	2.41 ± 0.01	2.34 ± 0.09	0.010	0.921
Total Grey Matter Volume [litre]	0.72 ± 0.08	0.72 ± 0.07	0.003	0.955
Total Intracranial Volume [litre]	1.45 ± 0.24	1.45 ± 0.21	0.000	0.994
	Biological Sex			
	Males (*n*=100)	Females (*n*=96)	*F*(*df*=1)	*p*
Age [years]	26.70 ± 6.41	27.60 ± 7.21	0.875	0.351
Full-scale IQ (WASI)	113.66 ± 11.57	116.59 ± 10.32	3.673	0.057
Verbal IQ	110.18 ± 11.98	117.21 ± 10.59	18.685	0.001*
Performance IQ	114.42 ± 12.49	112.45 ± 11.92	1.211	0.272
Mean Cortical Thickness [mm]	2.34 ± 0.085	2.33 ± 0.11	0.898	0.345
Total Grey Matter Volume [litre]	0.763 ± 0.06	0.677 ± 0.10	82.690	0.001*
Total Intracranial Volume [litre]	1.58 ± 0.19	1.32 ± 0.17	100.730	0.001*

Note. Data expressed as mean ± standard deviation; *F*,*p* resulting from a general linear model (GLM) including a main effect of diagnostic group and biological sex. * statistically significant based on $p < 0.05$ (two-sided)

eMethods. Supplementary Methods

Gaussian Process Classification of biological sex based on normative variability in CT

Gaussian process models were used for the probabilistic prediction of biological sex based on patterns of neuroanatomical variability in CT. Gaussian process classification (GPC) has previously been applied to MRI data [1,2], and a detailed description can be found in [3]. Briefly, we begin with a set of training data $X_{train}=\{X,y\}$, where X is an m x d matrix consisting of input vectors x_i (i.e. m training samples with d features each), and y is a column vector of target variables or class labels where $y_i \in \{-1, +1\}$. Training samples are indexed by $i = 1, \ldots, m$. The training data are used to estimate a probability distribution that allows us to predict a target y^* for a new data sample x^* as accurately as possible. For binary GPC, predictions take the form of predictive or 'class' probabilities, where the probability for a class results from $(y^*=1|x^*,X_{train})$. These predictions are computed by first estimating the posterior distribution of a set of vertex weights using the rules of probability, then passing the output through a sigmoid function to constrain the output to the unit interval, ensuring a valid probabilistic interpretation. The mode of the distribution of weights, $\boldsymbol{w}$, can be understood as providing a spatial representation of the decision boundary. If GPC is applied to neuroimaging data, $\boldsymbol{w}$ has the same number of elements as the feature vector $\boldsymbol{x}$, and can subsequently be used to create a map of the most important brain regions underlying the prediction (analogous to Support Vector Machine (SVM) discrimination maps).

Here, we initially employed GPC to establish (i.e. train) a predictive model of biological sex based on normative phenotypic variability in CT. Thus, the input matrix X was an $m \times d$ matrix of CT measures where m was defined as the number of typically developing (TD) controls (i.e. 51 males and 47 females), and d was defined as the number of vertices across the cortical surface. As target variable y, we used the class labels of -1 and +1 for neurotypical females and males respectively. This allowed us to

make probabilistic predictions for individuals based on the binary categories dictated by biological sex, utilizing their neuroanatomical brain phenotype. Class probabilities ranged from 0 to 1, wherein those being most confidently classified as phenotypically female (i.e. class probability=0) or male (i.e. class probability=1) representing the most prototypical (i.e. characteristic) male or female neurophenotype respectively. The GP classifier was trained by maximizing the logarithm of the marginal likelihood, which measures the total probability of the data given the Gaussian process prior and the model's hyperparameters [2]. The performance of the normative model was subsequently validated using cross validation, which provides robust parameter estimates of generalisation ability. Here, the classifier is trained repeatedly using all but one participant from each class label. This procedure was repeated *n* times, where *n* is the number of participants per class label. The accuracy of the classifier was measured by the proportion of observations that were correctly classified, e.g. the number of biological males (or females) correctly classified as male (or female) based on their brain phenotype. Permutation testing was used to assess the statistical significance of the model performance relative to chance level. To achieve this, we permuted the class (i.e. sex) labels 1000 times without replacement. Each time, the model was retrained and the accuracy was computed. All Gaussian process models were estimated using the GPML toolbox (www.guassianprocess.org/gpml/code).

The normative predictive model of biological sex was subsequently used to predict biological sex for the independent sample of ASD individuals. To visualize the spatially-distributed patterns of neuroanatomical variability in CT carrying high and low risk of ASD in males and females, we employed a recently proposed approach for mapping the contribution of each vertex to the classifier decision [1]. This approach has two advantages over the more conventional approach of mapping the weight vector: (1) it indicates the total contribution of each vertex to the prediction for each individual, i.e. not just the contribution from the training set; and (2) it can be used to map the neural constituents

for the predictions based on a second sample, independent from the training set (i.e. the clinical and normative samples respectively). To achieve this, we calculated the element-wise product of $\boldsymbol{w}$ and each individual's CT measures (i.e. x_i*CT) for (1) all males (or all females) classified as phenotypically male (i.e. class probability > 0.5), (2) all males (or all females) classified as phenotypically female (i.e. class probability < 0.5), and (3) across biological males and females with a class probability < 0.5 (or a class probability > 0.5). Within each of these groups and at each cerebral vertex, the resulting maps were then summarized by the mean value across individuals.

Estimation of ASD probability based on normative sex-related phenotypic variability of the brain

To determine whether normative sex-related variability in CT measures modulates the probability of ASD, we initially examined the (absolute) probability of ASD as a function of predictive probabilities for the TD male or female brain phenotype within our sample. The sample probability of ASD for females (or males) was determined as the ratio of females (or males) with ASD divided by the total number of females (or males) falling within eight bins (i.e. from 0 to 1 in steps of 0.125) along the axis of predictive class probabilities for the male neuroanatomical phenotype (*M*). Let *D* and *S* denote binary variables representing a diagnosis of ASD and biological sex respectively. This equals the posterior probability of having ASD (i.e. *D=1)* under the condition of being biologically female or male (i.e. *S*=0 or *S*=1, respectively), and given a neuroanatomical phenotype *M* quantified by class probabilities, so that $\mathbb{P}(D=1|M, S=s)$, for every $s \in \{0,1\}$.

Furthermore, this data allowed us to estimate the population risk of having a diagnosis of ASD, given that an individual exhibits a male or female neuroanatomical phenotype. In our notation, this may be expressed as $\mathbb{P}(D=1|M=m, S=s)$, for every $m \in \{0,1\}$ and $s \in \{0,1\}$ where 0 denotes female and 1 denotes male. Using Bayes theorem, such a conditional probability can be expressed as

$$\mathbb{P}(D = 1|M = m,\ S = s) = \frac{\mathbb{P}(M=m|D=1,S=s)\mathbb{P}(D=1|S=s)}{\mathbb{P}(M=m|S=s)}, \qquad (1)$$

in which the normalizing constant is obtained by integrating out *D*, so that $\mathbb{P}(M|D,S) = \mathbb{P}(M|D = 1,S)\mathbb{P}(D = 1|S) + \mathbb{P}(M|D = 0,S)\mathbb{P}(D = 0|S)$ for every realization of *M* and *S*. The probabilities in the numerator of the right-hand side of equation (1) are readily obtained from our sample, and from previous epidemiological studies (e.g. [4]). Indeed, the term $\mathbb{P}(M = m|D = 1,S = s)$ corresponds to the number of biological males or females with a diagnosis of ASD, who have been identified as having a male or female neuroanatomical phenotype by our GPC model.

Moreover, the prevalence rates of ASD for males and females in the general population (i.e. $\mathbb{P}(D=1|S=s)$) are known from epidemiological priors (i.e. 1:42 for males, 1:189 for females [4]). Based on these previous priors, and the sample estimates resulting from our study, we were therefore able to estimate the population risk of ASD given a male/female neuroanatomical phenotype for biological males and females, i.e. $\widehat{\mathbb{P}}(D|M,S)$. Note that the estimation of $\widehat{\mathbb{P}}(D = 1|M,S)$ presented here is analogous to the correction usually applied to a sensitivity test in order to compute the probability of having a disease, given a positive test result. In our context, the probability of a particular neuroanatomical phenotype can thus be regarded as a 'test' for disease status.

eFigure 1. Sex-Related Pattern of Neuroanatomical Variability in Cortical Thickness

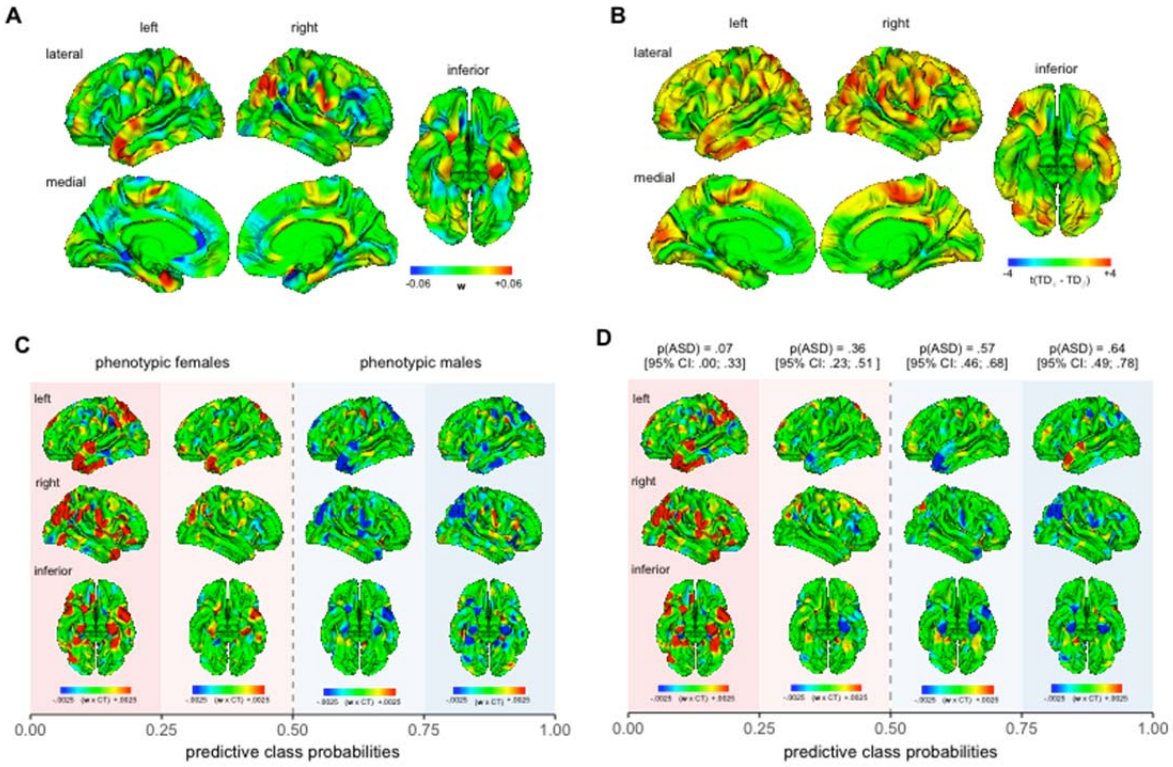

(**A**) Spatial distribution of the weight vector w resulting from the Gaussian Process Classification of biological sex in TD controls. (**B**) Un-thresholded statistical difference map representing t-test statistics resulting from the GLM-comparison between TD males and females using CT measures. Positive t-values (yellow to red colormap) indicate increased CT in TD females relative to males, while negative t-values (cyan to blue colormap) indicate decreased CT in females. Clusters with significant differences in CT following statistical thresholding are shown in eFigure 2 in the Supplement. (**C**) Patterns of normative neuroanatomical variability in CT associated with a phenotypic shift of the brain from a characteristic female to male presentation. These patterns were derived using a predictive mapping approach, which quantifies the extent to which the individual's neuroanatomy interacts with the weight vector ***w***. At each vertex, the color-scale therefore represents the product of ***w*** and CT, averaged across all individuals falling within four bins along the normative axis of predictive probabilities. (**D**) Patterns of sex-related neuroanatomical CT variability associated with high and low risk for ASD across sex categories. The risk of ASD was determined as the number of males and females with ASD relative to the total number of individuals falling within four intervals of predictive class probabilities. At each vertex, the color-scale indicates the product of ***w*** and CT, averaged across all individuals within the four risk groups. Brackets indicate the 95% confidence interval associated with the risk for ASD.

eFigure 2. Significant Differences in CT Between Male and Female TD Controls

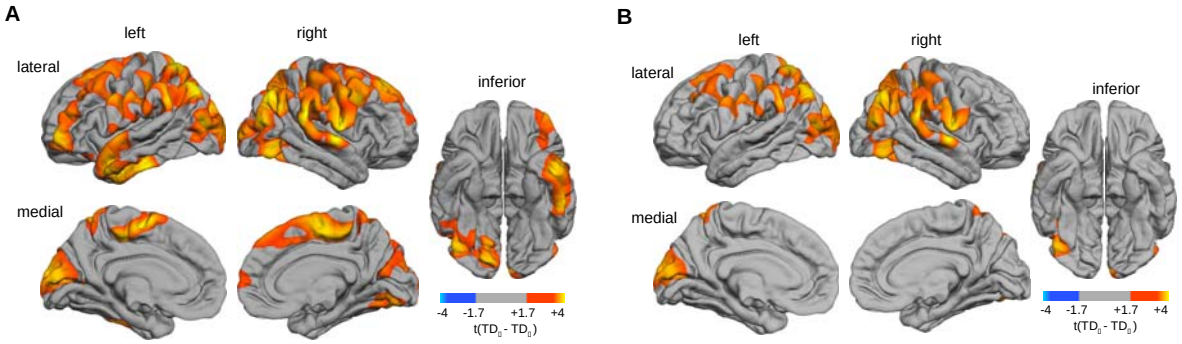

A) Clusters with significant between-group differences using random-field theory (RFT)-based clustering with a cluster threshold of 0.5 (two-tailed). The orange to yellow colormap indicates brain regions where CT is significantly increased in females relative to males. (**B**) Clusters with significant between-group differences using a non-parametric clustering approach with *n*=10,000 permutations at the same cluster-threshold and colormap.

eFigure 3. Sample Probability of ASD for Females (**A**) and Males (**B**) as a Function of Normative Sex-Related Phenotypic Variability in CT

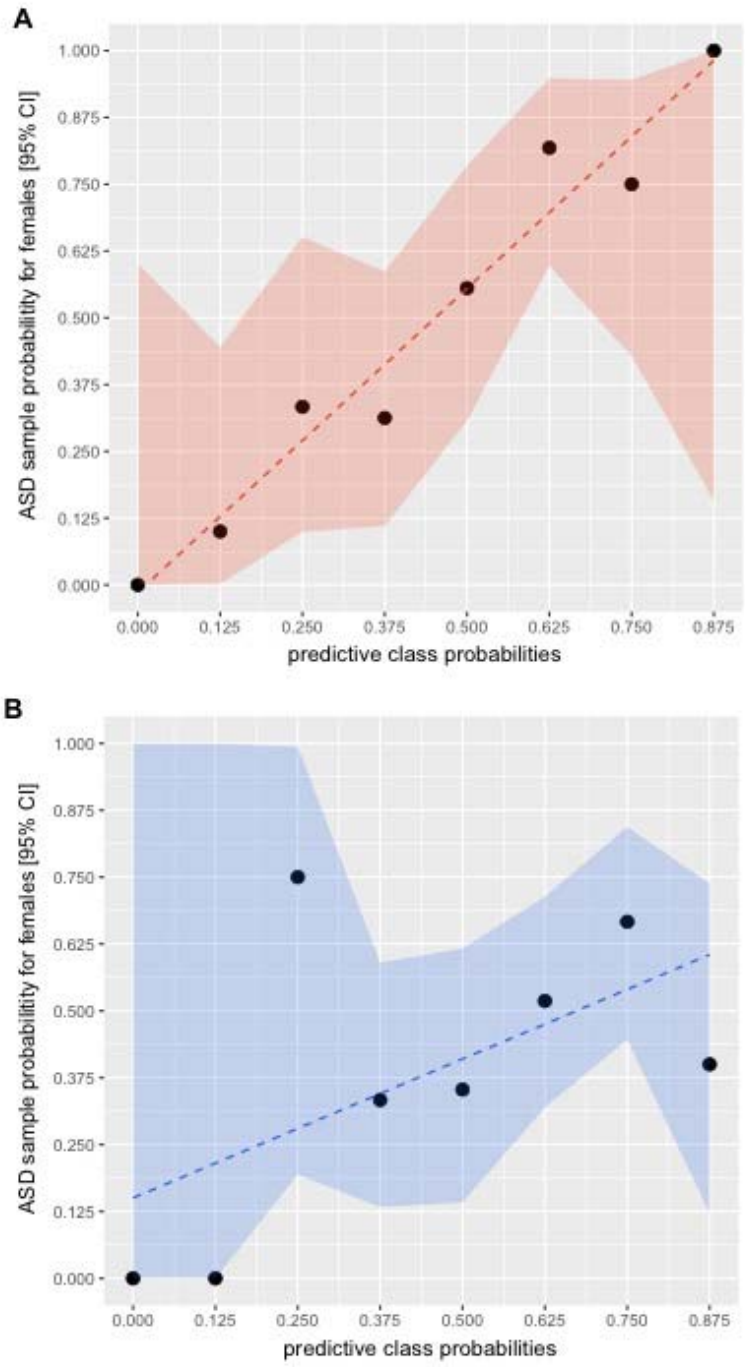

The sample probability of ASD was determined as the ratio of females (or males) with ASD relative to the total number of females (or males) falling within eight bins (i.e. from 0 to 1 in steps of 0.125) along the normative axis of predictive probabilities. The colored area around the regression line indicates the 95% confidence interval (CI) resulting from a binomial test, based on the hypothesis that the probability of having ASD is larger (or smaller) than the probability of not having ASD.

eFigure 4. Clusters With Significant Differences in the Neuroanatomical Pattern of CT Associated With High Probability of ASD Between Males and Females (i.e. Product of *w* and CT; See Figure 2 Right Panel)

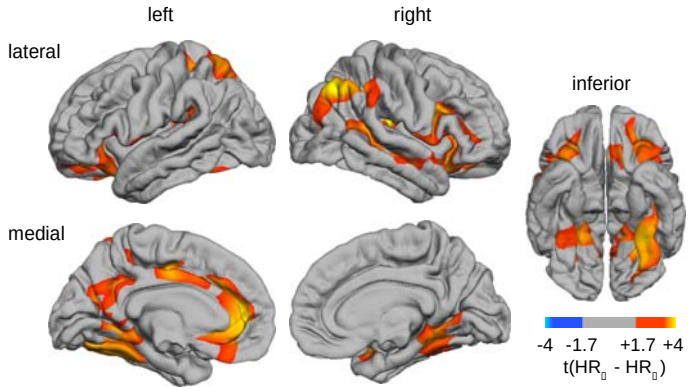

The red colormap indicates regions where females had a significant increased ***w*** x CT as compared to males (RFT-based cluster-corrected, $p<0.05$). There were no significant between-sex differences in the low ASD probability maps.

eFigure 5. Clusters With Significant Group-by-Sex Interactions Following a Non-parametric Clustering Approach With *n*=10,000 Permutations of Group (i.e. Sex) Labels (Permutation-Based Cluster-Corrected, $p<0.05$) (**A**). (**B**) Clusters where CT was significantly reduced in females with ASD relative to female controls (permutation-based cluster-corrected, $p<0.05$). No significant clusters remained when comparing ASD males with male TD controls using a permutation-based cluster correction.

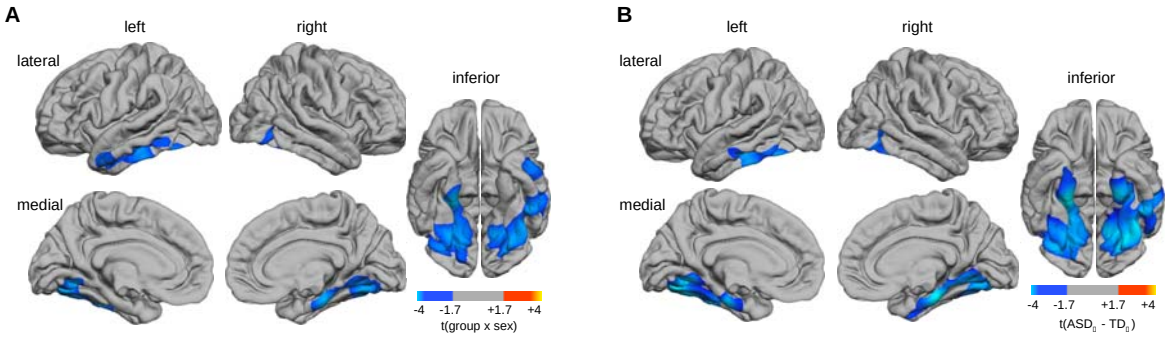

eFigure 6. Group-by-Sex Interaction Graph Based on Mean CT in the Left-Hemisphere Cluster That Extended Into the Hippocampal/Entorhinal Cortex, the Fusiform and Lingual Gyrus, and the Inferior/Middle Temporal Lobe (see cluster ID 1 in eTable 4)

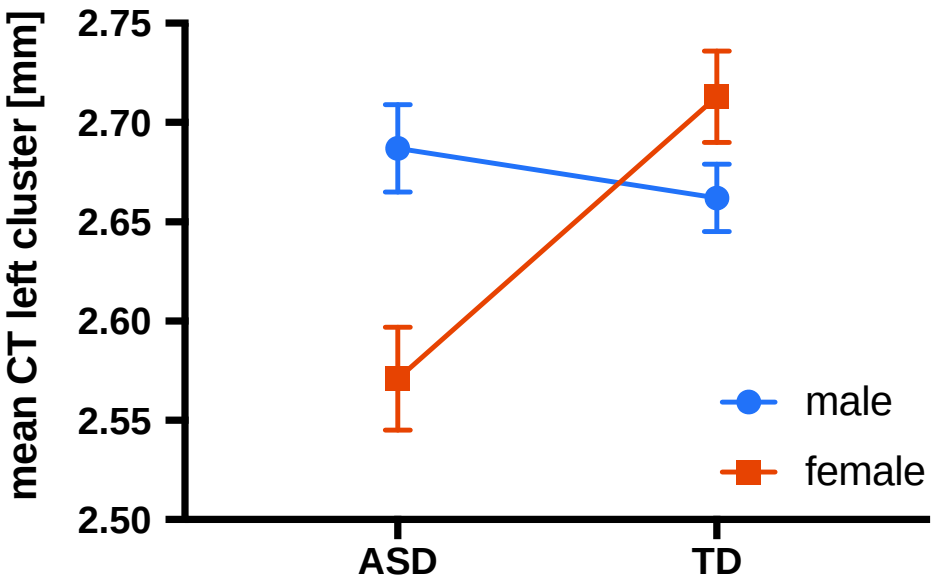

eFigure 7. Differences in Full-Scale, Verbal and Non-verbal (i.e. Performance) IQ Between Individual Subgroups of ASD vs. TD Individuals, and Males vs. Females, Examined Using *t* Tests for Independent Samples

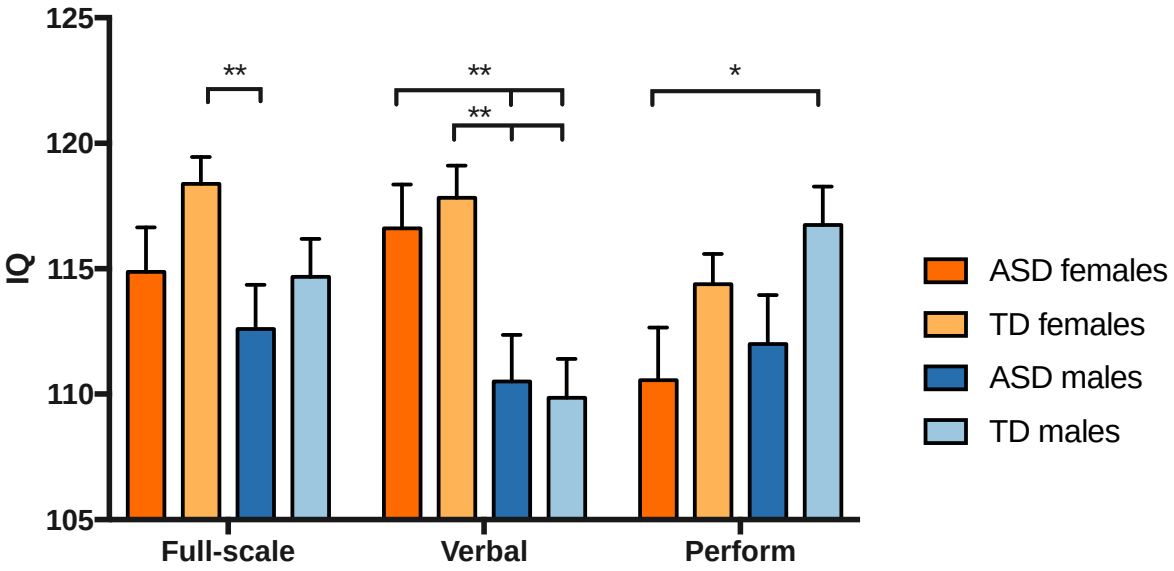

Note. ** indicates $p<0.01$, * indicates $p<0.05$.

eFigure 8. Spatially Distributed Pattern of Negative (Blue) and Positive (Red) Correlations Between Verbal IQ Measures and CT Assessed Across Male and Female Neurotypical Controls

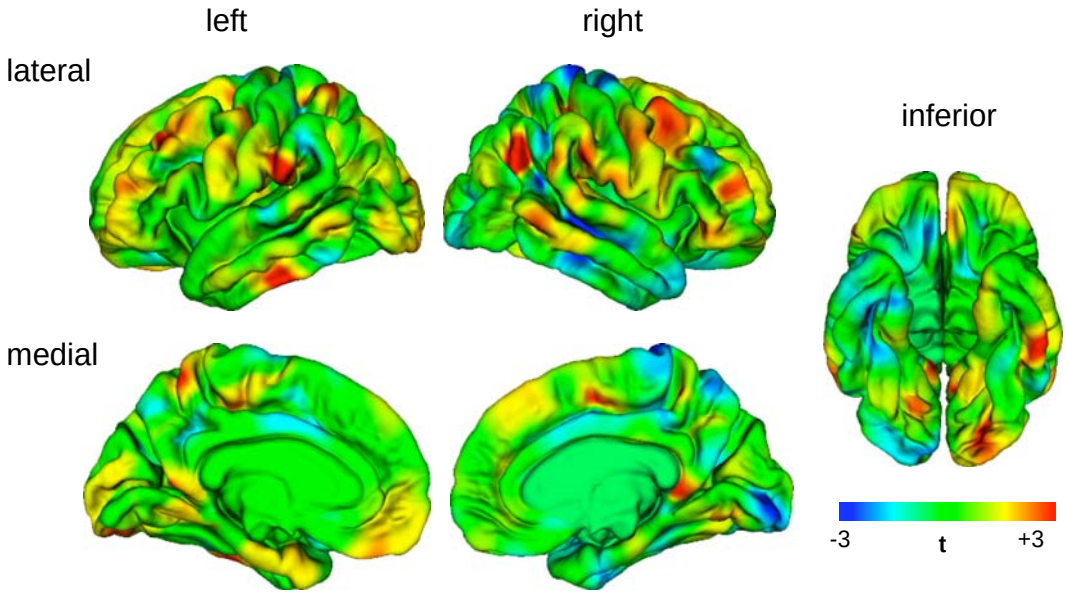

The colourmap indicates the *t* test statistics for vertex-wise correlation coefficients.

eAppendix. Supplementary Appendix

Relationship between sex-related neuroanatomical differences and inter-individual variability in clinical and/or neurocognitive measures

To determine how the observed sex-related differences in brain structure may be related to variability in clinical or neurocognitive measures, we also examined if differences in verbal and non-verbal (i.e. performance) IQ between diagnostic groups and biological sexes could explain the phenotypic shift of the brain in females. For example, neurotypical females tend to have a significantly higher verbal IQ than neurotypical males, which has previously been suggested to be a 'protective' factor for ASD (e.g. [5]). It is therefore possible that females with ASD display a neurocognitive profile that is more similar to the neurotypical male rather than female behavioral phenotype, which in turn could account for a more male-typic pattern of brain anatomy.

However, when examining similarities and differences in IQ measures between females with ASD, and male and female controls, we found that ASD females differed significantly from neurotypical males in both verbal ($t(97)=-2.993$, $p<0.01$) and performance IQ ($t(97)=2.406$, $p<0.05$). Moreover, ASD females were not statistically different from female controls ($p>0.05$, two-tailed) (see eFigure 7 in the Supplement). Based on IQ profiles, the ASD females assessed in our sample therefore seem functionally closer to female rather than male TD controls. Thus, based on IQ measures exclusively, our finding of increased predictive probabilities for the male neuroanatomical brain phenotype in ASD females seems to reflect a sex- rather than function-related difference in brain anatomy. Moreover, there was no significantly correlation between predictive probabilities for a male neuroanatomical brain phenotype and variability in verbal or performance IQ in females ($p>0.05$, two-tailed), as would be expected based on the absence of a significant difference between females with ASD and female controls. Given that females tend to have a significantly increased verbal IQ compared to males, we also compared the

normative patterns of neuroanatomical variability indicative of biological sex (i.e. the weight vector ***w***, eFigure 1a) with the spatially distributed pattern of correlations between CT measures and verbal IQ (see eFigure 8 in the Supplement). Overall, however, the distributed patterns indicative of biological sex, and the patterns associated with high and low ASD probability, are quite different from the spatial distribution of high/low correlations between CT and verbal IQ. Based on these findings, it seems unlikely that the results of our multivariate prediction of biological sex are driven by sex-dependent differences in verbal IQ, rather than by biological sex itself.

Last, we also explored the relationship between autistic symptoms and CT variability in the two main clusters with significant sex-by-group interactions (see Figure 3a) within the ASD group. Here, we utilized a GLM predicting CT variability using separate effects of biological sex and measures of symptom severity to (1) examine whether CT in these clusters is significantly correlated with measures of symptom severity within the ASD group, and to (2) disentangle the effect of biological sex from the effect of inter-individual variability in symptom severity. We examined these relationships in two separate statistical models, one including the three ADI-R subdomains, and one including the ADOS total and repetitive domain. Overall, we found that CT measures in the right-hemisphere cluster correlated with ADOS total scores exclusively ($r(97)=0.283$, $p<0.05$, two-tailed). No significant correlations were observed in the left-hemisphere cluster. However, when predicting CT by biological sex and ADOS total scores, both effects remained statistically significant in the right hemisphere ($p<0.05$, two-tailed). In the left hemisphere, only the effect of biological sex exceeded the level of statistical significance ($p<0.05$, two-tailed). Thus, while measures of symptom severity may explain some CT variability in addition biological sex, it seems that both effects are statistically separable. Although a more thorough investigation of this issue is required in the future, these preliminary results

indicate that our findings reflect neuroanatomical differences related to biological sex, and having a diagnosis of ASD, rather than functional differences in specific clinical or neurocognitive features.

eReferences. Supplementary References

1. Marquand AF, Brammer M, Williams SCR, Doyle OM. Bayesian multi-task learning for decoding multi-subject neuroimaging data. *Neuroimage*. 2014;92:298-311. doi:10.1016/j.neuroimage.2014.02.008.

2. Marquand A, Howard M, Brammer M, Chu C, Coen S, Mourão-Miranda J. Quantitative prediction of subjective pain intensity from whole-brain fMRI data using Gaussian processes. *Neuroimage*. 2010;49(3):2178-2189. doi:10.1016/j.neuroimage.2009.10.072.

3. Rasmussen C, Williams C. *Gaussian Processes for Machine Learning. Massachusetts Institute of Technology*. 2006.

4. Baio J. *Prevalence of Autism Spectrum Disorder Among Children Aged 8 Years—Autism and Developmental Disabilities Monitoring Network, Surveillance Summaries,* March 28, 2014, 63(SS02):1-21

5. Skuse DH, Mandy W, Steer C, Miller LL, Goodman R, Lawrence K, Emond A, Golding J. *Social communication competence and functional adaptation in general population of children: preliminary evidence for sex-by-verbal IQ differential risk.* J Am Acad Child Adolesc Psychiatry. 2009;48(2):128-137. doi:10.1097/CHI.0b013e31819176b8.